

# Constraints and Implications on Higgs FCNC Couplings from Precision Measurement of $B_s \rightarrow \mu^+ \mu^-$ Decay

Cheng-Wei Chiang,<sup>1,2,3,\*</sup> Xiao-Gang He,<sup>1,4,3,†</sup> Fang Ye,<sup>1,‡</sup> and Xing-Bo Yuan<sup>3,§</sup>

<sup>1</sup>*Department of Physics, National Taiwan University, Taipei 10617, Taiwan*

<sup>2</sup>*Institute of Physics, Academia Sinica, Taipei 11529, Taiwan*

<sup>3</sup>*Physics Division, National Center for Theoretical Sciences, Hsinchu 30013, Taiwan*

<sup>4</sup>*INPAC, Department of Physics and Astronomy,  
Shanghai Jiao Tong University, Shanghai 200240, China*

(Dated: November 15, 2017)

## Abstract

We study constraints and implications of the recent LHCb measurement of  $\mathcal{B}(B_s \rightarrow \mu^+ \mu^-)$  for tree-level Higgs-mediated flavor-changing neutral current (FCNC) interactions. Combined with experimental data on  $B_s$  mass difference  $\Delta m_s$ , the  $h \rightarrow \mu\tau$ , and the  $h \rightarrow \tau^+ \tau^-$  decay branching ratios from the LHC, we find that the Higgs FCNC couplings are severely constrained. The allowed regions for  $B_s \rightarrow \mu\tau$ ,  $\tau\tau$  and  $h \rightarrow sb$  decays are obtained. Current data allow large CP violation in the  $h \rightarrow \tau^+ \tau^-$  decay. Consequences of the Cheng-Sher ansatz for the Higgs Yukawa couplings are discussed in some detail.

---

\*e-mail: [chengwei@phys.ntu.edu.tw](mailto:chengwei@phys.ntu.edu.tw)

†e-mail: [hexg@phys.ntu.edu.tw](mailto:hexg@phys.ntu.edu.tw)

‡e-mail: [fangye@ntu.edu.tw](mailto:fangye@ntu.edu.tw)

§e-mail: [xbyuan@cts.nthu.edu.tw](mailto:xbyuan@cts.nthu.edu.tw)

## I. INTRODUCTION

The Standard Model (SM) of particle physics [1–6] has been working successfully to explain most phenomena observed in experiments. It reached its summit when the 125-GeV Higgs boson was discovered [7, 8] and its properties were later on shown to be in good agreement with SM expectations. An on-going program in particle physics is to determine at high precision the Higgs couplings with other SM particles, as such studies could reveal whether there is an extended Higgs sector and give us more information about electroweak symmetry breaking. If there is an extended Higgs sector, many observables in flavor physics that are sensitive to new physics (NP) can be affected.

In general, models with physics beyond the SM can lead to Higgs-mediated flavor-changing neutral currents (FCNC's) [9], which have severe constraints from flavor physics. Even though such FCNC's can be avoided by imposing certain conditions for natural flavor conservation [10] or Yukawa alignment [11], it is better to leave it to experimental data to tell us whether the FCNC couplings are indeed negligibly small or sufficiently sizeable to have some intriguing phenomenological effects.

One channel that provides an excellent probe for the Higgs-mediated FCNC couplings is the rare  $B_s \rightarrow \mu^+\mu^-$  decay [12–16]. This decay has a relatively simple structure in the SM, involving only a single vector current operator in the effective interaction Hamiltonian. Recently the LHCb Collaboration has measured a branching ratio  $\overline{\mathcal{B}}(B_s \rightarrow \mu^+\mu^-)_{\text{LHCb}} = (3.0 \pm 0.6^{+0.3}_{-0.2}) \times 10^{-9}$  for the  $B_s \rightarrow \mu^+\mu^-$  decay [17]. Combined with the previous CMS measurement  $\overline{\mathcal{B}}(B_s \rightarrow \mu^+\mu^-)_{\text{CMS}} = (3.0^{+1.0}_{-0.9}) \times 10^{-9}$  [18], one would obtain the average value

$$\overline{\mathcal{B}}(B_s \rightarrow \mu^+\mu^-)_{\text{avg}} = (3.0 \pm 0.5) \times 10^{-9} . \quad (1)$$

This value is in general agreement with the value predicted in the SM [19], which, using currently known inputs, is

$$\overline{\mathcal{B}}(B_s \rightarrow \mu^+\mu^-)_{\text{SM}} = (3.44 \pm 0.19) \times 10^{-9} . \quad (2)$$

Comparing the values above, one notices that the experimental central value is about 13% lower than the SM one. NP effects may address such a discrepancy, though the error bars are still too large to call for such a solution. Nevertheless one can use Eqs. (1) and (2) to constrain possible NP contributions and study their implications.

If the 125-GeV Higgs boson  $h$  has FCNC couplings to fermions, its mediation can produce scalar and/or pseudoscalar operators that contribute to the  $B_s \rightarrow \mu^+ \mu^-$  decay. In the SM, such operators are generated only at loop level and further suppressed by the small muon Yukawa coupling. However, such interactions may be generated at tree level and do not suffer from chiral suppression in physics beyond the SM. It is the primary purpose of this work to constrain such couplings using the recently measured  $B_s \rightarrow \mu^+ \mu^-$  decay along with others, and study the implications for other processes.

Another closely related and important constraint comes from the  $B_s$  mass difference through the  $B_s$ - $\bar{B}_s$  mixing effect. The updated SM prediction of  $\Delta m_s$  [20] and the most recent experimental measurement [21] are, respectively,

$$\Delta m_s^{\text{SM}} = (18.64_{-2.27}^{+2.40}) \text{ ps}^{-1}, \quad \Delta m_s^{\text{exp}} = (17.757 \pm 0.021) \text{ ps}^{-1}. \quad (3)$$

They provide a tight constraint on tree-level Higgs scalar and pseudoscalar couplings with the  $s$  and  $b$  quarks.

In the lepton sector, a hint of significant flavor-changing Higgs couplings comes from recent measurements of

$$\mathcal{B}(h \rightarrow \mu\tau)_{\text{CMS}} = (0.84_{-0.37}^{+0.39})\% [22], \quad \mathcal{B}(h \rightarrow \mu\tau)_{\text{ATLAS}} = (0.53 \pm 0.51)\% [23] \quad (4)$$

obtained by the CMS and ATLAS Collaborations, respectively. The central values of such large branching ratios, if taken seriously, call for a sizeable  $\mu$ - $\tau$  flavor-violating Higgs coupling.

The existence of FCNC couplings of the Higgs boson to fermions occur in many extensions of the SM in the Higgs sector [24], such as multi-Higgs doublet models [9]. A simple example that can lead to tree level Higgs FCNC couplings with fermions is by introducing certain dimension-6 operators [25]:

$$\frac{\phi^\dagger \phi}{\Lambda^2} \bar{\ell}_{Li} g_{ij}^l \phi e_{Rj}, \quad \frac{\phi^\dagger \phi}{\Lambda^2} \bar{Q}_{Li} g_{ij}^d \phi D_{Rj}, \quad \frac{\phi^\dagger \phi}{\Lambda^2} \bar{Q}_{Li} g_{ij}^u \tilde{\phi} U_{Rj}, \quad (5)$$

where  $\Lambda$  denotes some new physics scale, in addition to the usual dimension-4 Yukawa interactions  $\bar{\ell}_{Li} y_{ij}^u \phi e_{Rj}$ ,  $\bar{Q}_{Li} y_{ij}^d \phi D_{Rj}$ , and  $\bar{Q}_{Li} y_{ij}^u \tilde{\phi} U_{Rj}$ . Here  $\ell_{Li}$  denote the left-handed leptons,  $Q_{Li}$  the left-handed quarks,  $e_{Ri}$  the right-handed charged leptons,  $D_{Ri}$  the right-handed down-type quarks,  $U_{Ri}$  the right-handed up-type quarks,  $\phi$  the Higgs doublet, and  $\tilde{\phi} \equiv i\sigma_2 \phi^*$ .

In the mass eigenbasis, Higgs FCNC interactions will be generated by the term  $\delta Y^f = (v^2/2\Lambda^2)(S_L^\dagger g^f S_R)$  induced by the above-mentioned dimension-6 operators, where  $S_L$  and

$S_R$  denote respectively the bi-unitary transformation matrices for the left-handed and right-handed fermion fields to obtain the diagonal fermion mass matrix  $\hat{M}$ . As a result, the Yukawa interaction Lagrangian in the mass eigenbasis is given by

$$\mathcal{L}_{h\bar{f}f} \equiv -\frac{1}{\sqrt{2}}\bar{f}(Y^f + i\gamma_5\bar{Y}^f)fh, \quad (6)$$

where  $Y^f = \sqrt{2}\hat{M}^f/v + (\delta Y^f + \delta Y^{f\dagger})$  and  $\bar{Y}^f = -i(\delta Y^f - \delta Y^{f\dagger})$  are in general non-diagonal and  $v = 246$  GeV is the vacuum expectation value of the SM Higgs field. Hence, they can induce Higgs-mediated FCNC processes at tree level.

In this work, we make use of the combined result of the  $B_s \rightarrow \mu^+\mu^-$  branching ratio, the  $B_s$  mass difference (3), and the  $h \rightarrow \tau\tau$  [26] and  $h \rightarrow \mu\tau$  [22, 23] decay rates to constrain the involved Higgs couplings. From the constrained parameter space, we can make predictions for the  $B_s \rightarrow \mu^\pm\tau^\mp$  and  $\tau^+\tau^-$  as well as the  $h \rightarrow sb$  decays without invoking additional assumptions.

Generically elements in the Yukawa matrices  $Y^f$  and  $\bar{Y}^f$  are independent of each other. In order to increase the predictive power, one often employs some texture for the Yukawa couplings, such as the Cheng-Sher ansatz [27], so that one can also compute the rates for more related processes. We will take the Cheng-Sher ansatz as a working assumption to put it to a test in the face of the coupling constraints extracted from the above-mentioned data.

The structure of this paper is as follows. In Section II, we discuss how the tree-level Higgs-mediated FCNC interactions affect the  $B_s \rightarrow \mu^+\mu^-$  decay, the  $B_s$ - $\bar{B}_s$  mixing, and the  $h \rightarrow \mu\tau$  and  $\tau\tau$  decays. In Section III, we present a detailed numerical analysis to obtain the allowed parameter space for the FCNC couplings. In Section IV, we first study implications for the  $h \rightarrow \mu\tau$  and  $B_s \rightarrow \mu\tau$ ,  $\tau\tau$  decays without invoking any additional assumptions. We then estimate more related observables by taking the Cheng-Sher ansatz. We draw conclusions in Section V.

## II. THEORETICAL FRAMEWORK

In this section, we discuss how the Higgs Yukawa couplings given in Eq. (6) affect the processes of interest to us; namely, the  $B_s \rightarrow \mu^+\mu^-$  decay, the  $B_s$  mass difference, and the  $h \rightarrow \mu\tau$  and  $sb$  decays.

### A. The $B_s \rightarrow \mu^+ \mu^-$ decay

With the Higgs exchanges introduced in the previous section and the SM contribution, the effective Hamiltonian responsible for the  $\bar{B}_s \rightarrow \mu^+ \mu^-$  decay is given by [28]

$$\mathcal{H}_{\text{eff}} = -\frac{G_F}{\sqrt{2}} \frac{\alpha_{em}}{\pi s_W^2} V_{tb} V_{ts}^* (C_A \mathcal{O}_A + C_S \mathcal{O}_S + C_P \mathcal{O}_P + C'_S \mathcal{O}'_S + C'_P \mathcal{O}'_P) + h.c., \quad (7)$$

where  $\alpha_{em}$  is the fine structure constant, and  $s_W^2 \equiv \sin^2 \theta_W$  with  $\theta_W$  being the weak mixing angle.  $V_{ij}$  denote the Cabibbo-Kobayashi-Maskawa (CKM) matrix elements. The operators  $\mathcal{O}_i^{(\prime)}$  are defined as

$$\begin{aligned} \mathcal{O}_A &= (\bar{q} \gamma_\mu P_L b) (\bar{\mu} \gamma^\mu \gamma_5 \mu), & \mathcal{O}_S &= m_b (\bar{q} P_R b) (\bar{\mu} \mu), & \mathcal{O}_P &= m_b (\bar{q} P_R b) (\bar{\mu} \gamma_5 \mu), \\ \mathcal{O}'_S &= m_b (\bar{q} P_L b) (\bar{\mu} \mu), & \mathcal{O}'_P &= m_b (\bar{q} P_L b) (\bar{\mu} \gamma_5 \mu), \end{aligned} \quad (8)$$

where the  $b$  quark mass  $m_b$  is included in the definition of  $\mathcal{O}_{S,P}^{(\prime)}$  so that their Wilson coefficients are renormalization group invariant [12].

In the framework we are working with, the Wilson coefficient  $C_A$  contains only the SM contribution, and its explicit expression up to the NLO QCD corrections can be found in Refs. [29–31]. Recently, corrections at the NLO EW [32] and NNLO QCD [33] have been completed, with the numerical value approximated by [19]

$$C_A^{\text{SM}}(\mu_b) = -0.4690 \left( \frac{m_t^{\text{P}}}{173.1 \text{ GeV}} \right)^{1.53} \left( \frac{\alpha_s(m_Z)}{0.1184} \right)^{-0.09}, \quad (9)$$

where  $m_t^{\text{P}}$  denotes the top-quark pole mass. In the SM, the Wilson coefficients  $C_S^{\text{SM}}$  and  $C_P^{\text{SM}}$  can be induced by the Higgs-penguin diagrams but are highly suppressed. Their expressions can be found in Refs. [34, 35]. As a very good approximation, we can safely take  $C_S^{\text{SM}} = C'_S^{\text{SM}} = C_P^{\text{SM}} = C'_P^{\text{SM}} = 0$ .

With the Higgs-mediated FCNC interactions in the effective Lagrangian, Eq. (6), the scalar and pseudoscalar Wilson coefficients

$$\begin{aligned} C_S^{\text{NP}} &= \kappa (Y_{sb} + i \bar{Y}_{sb}) Y_{\mu\mu}, & C_P^{\text{NP}} &= i \kappa (Y_{sb} + i \bar{Y}_{sb}) \bar{Y}_{\mu\mu}, \\ C'_S^{\text{NP}} &= \kappa (Y_{sb} - i \bar{Y}_{sb}) Y_{\mu\mu}, & C'_P^{\text{NP}} &= i \kappa (Y_{sb} - i \bar{Y}_{sb}) \bar{Y}_{\mu\mu}, \end{aligned} \quad (10)$$

where the common factor

$$\kappa = \frac{\pi^2}{2G_F^2} \frac{1}{V_{tb} V_{ts}^*} \frac{1}{m_b m_h^2 m_W^2}. \quad (11)$$

For the effective Hamiltonian Eq. (7), the branching ratio of  $B_s \rightarrow \mu^+ \mu^-$  reads [34, 35]

$$\mathcal{B}(B_s \rightarrow \mu^+ \mu^-) = \frac{\tau_{B_s} G_F^4 m_W^4}{8\pi^5} |V_{tb} V_{tq}^*|^2 f_{B_s}^2 m_{B_s} m_\mu^2 \sqrt{1 - \frac{4m_\mu^2}{m_{B_s}^2} (|P|^2 + |S|^2)}, \quad (12)$$

where  $m_{B_s}$ ,  $\tau_{B_s}$  and  $f_{B_s}$  denotes the mass, lifetime and decay constant of the  $B_s$  meson, respectively. The amplitudes  $P$  and  $S$  are defined as

$$\begin{aligned} P &\equiv C_A + \frac{m_{B_s}^2}{2m_\mu} \left( \frac{m_b}{m_b + m_s} \right) (C_P - C'_P), \\ S &\equiv \sqrt{1 - \frac{4m_\mu^2}{m_{B_s}^2}} \frac{m_{B_s}^2}{2m_\mu} \left( \frac{m_b}{m_b + m_s} \right) (C_S - C'_S). \end{aligned} \quad (13)$$

Note that the NP scalar operators (*i.e.*, the  $\bar{Y}_{sb} Y_{\mu\mu}$  term) contribute to the branching ratio incoherently and always increase the latter, while the NP pseudoscalar operators (*i.e.*, the  $\bar{Y}_{sb} \bar{Y}_{\mu\mu}$  term) have interference with the SM amplitude and the resulting effects may be constructive or destructive, depending on the sign of  $\bar{Y}_{sb} \bar{Y}_{\mu\mu}$ . Given that the experimental value of the branching ratio is lower than that predicted by the SM, we expect the  $\bar{Y}_{sb} \bar{Y}_{\mu\mu}$  parameter to play the role of reducing the  $B_s \rightarrow \mu^+ \mu^-$  theoretical value to the experimental level.

Due to the  $B_s$ - $\bar{B}_s$  oscillations, the measured branching ratio of  $B_s \rightarrow \mu^+ \mu^-$  should be the time-integrated one [13]:

$$\bar{\mathcal{B}}(B_s \rightarrow \mu^+ \mu^-) = \left( \frac{1 + \mathcal{A}_{\Delta\Gamma} y_s}{1 - y_s^2} \right) \mathcal{B}(B_s \rightarrow \mu^+ \mu^-), \quad (14)$$

where [15]

$$y_s = \frac{\Gamma_s^L - \Gamma_s^H}{\Gamma_s^L + \Gamma_s^H} = \frac{\Delta\Gamma_s}{2\Gamma_s} \quad \text{and} \quad \mathcal{A}_{\Delta\Gamma} = \frac{|P|^2 \cos(2\varphi_P - \phi_s^{\text{NP}}) - |S|^2 \cos(2\varphi_S - \phi_s^{\text{NP}})}{|P|^2 + |S|^2}, \quad (15)$$

$\Gamma_s^L$  and  $\Gamma_s^H$  denote respectively the decay widths of the light and heavy  $B_s$  mass eigenstates, and  $\varphi_P$  and  $\varphi_S$  are the phases associated with  $P$  and  $S$ , respectively. The CP phase  $\phi_s^{\text{NP}}$  comes from  $B_s$ - $\bar{B}_s$  mixing and will be defined in eq. (21). In the SM,  $\mathcal{A}_{\Delta\Gamma}^{\text{SM}} = 1$ .

## B. The mass difference $\Delta m_s$

If  $Y_{sb}$  and/or  $\bar{Y}_{sb}$  are non-zero, contributions to  $B_s$ - $\bar{B}_s$  mixing can be induced. Therefore, one must make sure that the current measurement of mass difference  $\Delta m_s$  is respected. In the SM,  $B_s$ - $\bar{B}_s$  mixing occurs mainly via the box diagrams involving the exchange of  $W^\pm$

bosons and top quarks. The mass difference between the two mass eigenstates  $B_s^H$  and  $B_s^L$  can be obtained from the  $\Delta B = 2$  effective Hamiltonian [36]

$$\mathcal{H}_{\text{eff}}^{\Delta B=2} = \frac{G_F^2}{16\pi^2} m_W^2 (V_{tb} V_{ts}^*)^2 \sum_i C_i \mathcal{O}_i + \text{h.c.} , \quad (16)$$

where the operators relevant to our study are

$$\begin{aligned} \mathcal{O}_1^{\text{VLL}} &= (\bar{s}^\alpha \gamma_\mu P_L b^\alpha) (\bar{s}^\beta \gamma^\mu P_L b^\beta) , & \mathcal{O}_1^{\text{SLL}} &= (\bar{s}^\alpha P_L b^\alpha) (\bar{s}^\beta P_L b^\beta) , \\ \mathcal{O}_2^{\text{LR}} &= (\bar{s}^\alpha P_L b^\alpha) (\bar{s}^\beta P_R b^\beta) , & \mathcal{O}_1^{\text{SRR}} &= (\bar{s}^\alpha P_R b^\alpha) (\bar{s}^\beta P_R b^\beta) , \end{aligned} \quad (17)$$

with  $\alpha$  and  $\beta$  color indices. The SM contributes only the  $\mathcal{O}_1^{\text{VLL}}$  operator, with the corresponding Wilson coefficient at the LO given by [37]

$$C_1^{\text{VLL,SM}}(\mu_W) \approx 9.84 \left( \frac{m_t}{170 \text{ GeV}} \right)^{1.52} , \quad (18)$$

whose analytical expression can be found in Ref. [28].

With the effective Lagrangian in Eq. (6), the tree-level Higgs exchange results in

$$\begin{aligned} C_1^{\text{SLL,NP}} &= -\frac{1}{2} \tilde{\kappa} (Y_{sb} - i\bar{Y}_{sb})^2 , & C_2^{\text{LR,NP}} &= -\tilde{\kappa} (Y_{sb}^2 + \bar{Y}_{sb}^2) , \\ C_1^{\text{SRR,NP}} &= -\frac{1}{2} \tilde{\kappa} (Y_{sb} + i\bar{Y}_{sb})^2 , & \tilde{\kappa} &= \frac{8\pi^2}{G_F^2} \frac{1}{m_h^2 m_W^2} \frac{1}{(V_{tb} V_{ts}^*)^2} . \end{aligned} \quad (19)$$

The contribution from  $\mathcal{H}_{\text{eff}}^{\Delta B=2}$  to the transition matrix element of  $B_s - \bar{B}_s$  mixing is given by [36],

$$M_{12}^s = \langle B_s | \mathcal{H}_{\text{eff}}^{\Delta B=2} | \bar{B}_s \rangle = \frac{G_F^2}{16\pi^2} m_W^2 (V_{tb} V_{ts}^*)^2 \sum C_i \langle B_s | \mathcal{O}_i | \bar{B}_s \rangle , \quad (20)$$

where recent lattice calculations of the hadronic matrix elements  $\langle \mathcal{O}_i \rangle$  can be found in Refs. [38, 39]. Then the mass difference and CP violation phase read

$$\Delta m_s = 2 |M_{12}^s| , \quad \text{and} \quad \phi_s = \arg M_{12}^s . \quad (21)$$

In the case of complex Yukawa couplings,  $\phi_s$  can deviate from the SM prediction, i.e.,  $\phi_s = \phi_s^{\text{SM}} + \phi_s^{\text{NP}}$ . Nonzero  $\phi_s^{\text{NP}}$  can affect the CP violation in the  $B_s \rightarrow J/\psi\phi$  decay [20], as well as  $\mathcal{A}_{\Delta\Gamma}$  in the  $B_s \rightarrow \mu^+ \mu^-$  decay as in eq. (15). We note that  $\Delta m_s$  depends only on  $Y_{sb}^2$  and  $\bar{Y}_{sb}^2$ , but not  $Y_{sb} \bar{Y}_{sb}$ . In addition, the renormalization group evolution of the NP operators  $\mathcal{O}_1^{\text{SLL}}$ ,  $\mathcal{O}_1^{\text{SRR}}$  and  $\mathcal{O}_2^{\text{LR}}$  has been investigated in detail in Ref. [36]. Its effects are found to be small and therefore neglected in the following analysis.

### C. The $h \rightarrow f_1 f_2$ decays

The partial width of the Higgs boson decaying to a pair of fermions in the Born approximation is given by

$$\Gamma(h \rightarrow f_1 f_2) = S N_c \frac{m_h}{8\pi} (|Y_{f_1 f_2}|^2 + |\bar{Y}_{f_1 f_2}|^2) , \quad (22)$$

where  $S = 1$  ( $1/2$ ) when  $f_1$  and  $f_2$  are of different (same) flavors and  $N_c$  denotes the number of colors for the fermions.

With the pseudoscalar Yukawa couplings also included in our analysis, one can consider the possibility of observing CP violation in  $h \rightarrow \tau^+ \tau^-$  through the operator  $\mathcal{O}_\pi = \vec{p}_\tau \cdot (\vec{p}_{\pi^+} \times \vec{p}_{\pi^-})$ . Here  $\vec{p}_{\pi^+}$  and  $\vec{p}_{\pi^-}$  are respectively the 3-momenta of  $\pi^+$  and  $\pi^-$  from the  $\tau^+ \rightarrow \pi^+ \bar{\nu}_\tau$  and  $\tau^- \rightarrow \pi^- \nu_\tau$  decay, and  $\vec{p}_\tau$  is the momentum of the  $\tau^-$  from  $h \rightarrow \tau^+ \tau^-$  decay. Letting  $N_+$  and  $N_-$  be events with  $\mathcal{O}_\pi > 0$  and  $\mathcal{O}_\pi < 0$ , respectively, one can define a CP violating observable

$$A_\pi = \frac{N_+ - N_-}{N_+ + N_-} \approx \frac{\pi (Y_{\tau\tau} \bar{Y}_{\tau\tau})}{4 Y_{\tau\tau}^2 + \bar{Y}_{\tau\tau}^2} , \quad (23)$$

which can be measured experimentally [40].

### III. NUMERICAL ANALYSIS

With the theoretical formalism discussed in the previous sections and the input parameters given in Table I, we can compare relevant SM predictions with the recent experimental measurements to see if any NP is allowed. At present, the theoretical uncertainties for  $B_s \rightarrow \mu^+ \mu^-$  and  $\Delta m_s$  mainly arise from the decay constant  $f_{B_s}$  and the CKM matrix element  $|V_{cb}|$ . As is well known, there is a long-standing tension between the inclusive and exclusive determinations of  $|V_{cb}|$  and  $|V_{ub}|$  [41]. We find that the branching ratio obtained from the exclusive  $|V_{cb}|$  and  $|V_{ub}|$  are about 10% smaller than the one from the inclusive values, mainly due to the difference in  $|V_{cb}|$ . Here we adopt the recent average given by the CKMfitter group [42]. For the lifetime, both  $\Gamma_s^H$  and  $\Delta\Gamma_s/\Gamma_s$  are used. The SM prediction then depends only on  $\Gamma_s^H$ . Finally, compared to the SM prediction of  $(3.65 \pm 0.23) \times 10^{-9}$  previously given in Ref. [19], our theoretical uncertainty is smaller mainly due to more precise values of  $f_{B_s}$  and  $\Gamma_s^H$ .

Input	Value	Unit	Ref.
$\alpha_s^{(5)}(m_Z)$	$0.1181 \pm 0.0011$		[41]
$1/\alpha_{\text{em}}^{(5)}(m_Z)$	$127.944 \pm 0.014$		[41]
$m_t^{\text{P}}$	$173.21 \pm 0.51 \pm 0.71$	GeV	[41]
$ V_{cb} $ (semi-leptonic)	$41.00 \pm 0.33 \pm 0.74$	$10^{-3}$	[42]
$ V_{ub} $ (semi-leptonic)	$3.98 \pm 0.08 \pm 0.22$	$10^{-3}$	[42]
$ V_{us} f_+^{K \rightarrow \pi}(0)$	$0.2165 \pm 0.0004$		[42]
$\gamma$	$72.1_{-5.8}^{+5.4}$	[°]	[42]
$f_+^{K \rightarrow \pi}(0)$	$0.9681 \pm 0.0014 \pm 0.0022$		[42]
$f_{B_s}$	$228.4 \pm 3.7$	MeV	[43]
$f_{B_s} \sqrt{\widehat{B}}$	$270 \pm 16$	MeV	[43]
$1/\Gamma_s^{\text{H}}$	$1.609 \pm 0.010$	ps	[21]
$\Delta\Gamma_s/\Gamma_s$	$0.129 \pm 0.009$		[21]

TABLE I: Inputs for  $B_s \rightarrow \mu^+ \mu^-$  and  $B_s$ - $\bar{B}_s$  mixing.

For the  $B_s$ - $\bar{B}_s$  mixing, the SM prediction of  $\Delta m_s$  in Ref. [20] is updated with the input parameters in Table I, and reads in comparison with the most recent experimental measurement (3). Note that the SM central value is larger than the experimental one. Hence we expect the NP amplitude to interfere with the SM amplitude destructively. We will see later that this results in an upper bound of the Yukawa couplings  $|\bar{Y}_{sb}|$  and  $|Y_{sb}|$ .

In the following, we carry out numerical analysis for constraints on the Yukawa couplings from  $B_s \rightarrow \mu^+ \mu^-$  and  $B_s$ - $\bar{B}_s$  mixing. The allowed parameter space of these Yukawa couplings from each of the observables is obtained by requiring that the difference between the theoretical prediction and experimental measurement be less than twice the error bar (i.e. 95% confidence level (CL).), calculated by adding the theoretical and experimental errors in quadrature. This requirement implies the following bound from the  $B_s \rightarrow \mu^+ \mu^-$  decay branching ratio:

$$0.66 \lesssim |5.6 \times 10^5 \bar{Y}_{sb} Y_{\mu\mu}|^2 + |1 - 6.0 \times 10^5 \bar{Y}_{sb} \bar{Y}_{\mu\mu}|^2 \lesssim 1.26. \quad (24)$$

For illustration purposes, we take  $Y_{sb}$  and  $\bar{Y}_{sb}$  to be real, and plot the allowed region for  $\bar{Y}_{sb} Y_{\mu\mu}$  and  $\bar{Y}_{sb} \bar{Y}_{\mu\mu}$  in Fig. 1.

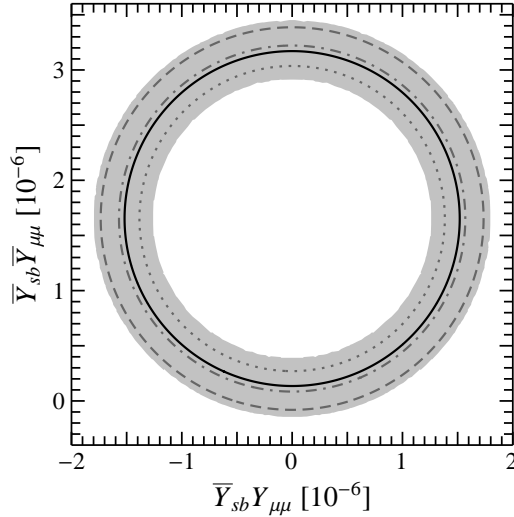


FIG. 1: Allowed parameter space in the  $(\bar{Y}_{sb}Y_{\mu\mu}, \bar{Y}_{sb}\bar{Y}_{\mu\mu})$  plane as constrained by the  $B_s \rightarrow \mu^+\mu^-$  decay. The black solid curve and the shaded region correspond respectively to the central value and the allowed region at 95% CL. The dashed, dot-dashed and dotted contours correspond to  $\bar{\mathcal{B}}(B_s \rightarrow \mu^+\mu^-)/\bar{\mathcal{B}}(B_s \rightarrow \mu^+\mu^-)_{\text{SM}} = 1.1, 0.9$  and  $0.7$ , respectively.

In Fig. 1, the allowed region is the shaded elliptical ring, as constrained by the combined CMS and LHCb measurement of  $\bar{\mathcal{B}}(B_s \rightarrow \mu^+\mu^-)$  at the 95% CL. With the contributions from the Higgs FCNC Lagrangian in Eq. (6), the branching ratio of  $B_s \rightarrow \mu^+\mu^-$  depends on two parameters:  $\bar{Y}_{sb}Y_{\mu\mu}$  and  $\bar{Y}_{sb}\bar{Y}_{\mu\mu}$ . As discussed in the previous section, the NP pseudoscalar operator  $\mathcal{O}_P^{\text{NP}}$  (*i.e.*, the  $\bar{Y}_{sb}\bar{Y}_{\mu\mu}$  contribution) has either constructive or destructive interference with the SM amplitude, while the NP scalar operator  $\mathcal{O}_S^{\text{NP}}$  (*i.e.*, the  $\bar{Y}_{sb}Y_{\mu\mu}$  contribution) always enhances the branching ratio. Therefore, in the region of small  $\bar{Y}_{sb}Y_{\mu\mu}$  and  $\bar{Y}_{sb}\bar{Y}_{\mu\mu}$ , the branching ratio is much more sensitive to the parameter  $\bar{Y}_{sb}Y_{\mu\mu}$  than to  $\bar{Y}_{sb}\bar{Y}_{\mu\mu}$ . It is also noted that the current experimental central value  $\bar{\mathcal{B}}(B_s \rightarrow \mu^+\mu^-)_{\text{avg}}/\bar{\mathcal{B}}(B_s \rightarrow \mu^+\mu^-)_{\text{SM}} \approx 0.87$ .

Fig. 2 shows the constraints in the  $(Y_{sb}, \bar{Y}_{sb})$  plane from the  $B_s$ - $\bar{B}_s$  mixing, assuming the two Yukawa couplings to be real. As mentioned earlier, we find two shaded regions that agree with the experimental measurement at 95% CL. Near the origin in the parameter space, the Higgs-mediated FCNC effects are mostly destructive with the SM contributions. From  $\Delta m_s$  alone, the pseudoscalar coupling  $\bar{Y}_{sb}$  has the bound

$$|\bar{Y}_{sb}| \lesssim 5 \times 10^{-4} \quad \text{or} \quad 1.1 \times 10^{-3} \lesssim |\bar{Y}_{sb}| \lesssim 1.4 \times 10^{-3} \quad (25)$$

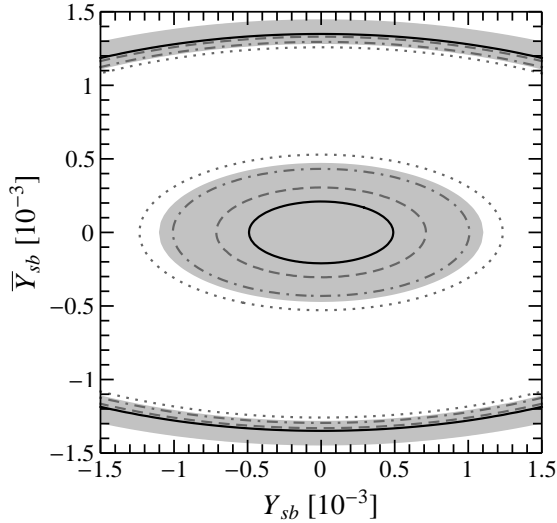


FIG. 2: Allowed parameter space in the  $(Y_{sb}, \bar{Y}_{sb})$  plane as constrained by the  $B_s$ - $\bar{B}_s$  mixing. The black solid curve and the shaded region correspond respectively to the central value and the 95%-CL region of the measured  $\Delta m_s$ . The dashed, dot-dashed, and dotted contours correspond to  $\Delta m_s/\Delta m_s^{\text{SM}} = 0.9, 0.8$  and  $0.7$ , respectively. The outer elliptical ring corresponds to the case where the Higgs-mediated FCNC interactions dominate over the SM contribution, thus flipping the sign of  $M_{12}^s$ .

at 95% CL. Taking  $|\bar{Y}_{sb}| = 5 \times 10^{-4}$  as an example, we find that the couplings  $Y_{\mu\mu}$  and  $\bar{Y}_{\mu\mu}$  are of  $\mathcal{O}(10^{-3})$ , comparable to the SM muon Yukawa coupling  $\lambda_\mu = \sqrt{2}m_\mu/v \approx 6.1 \times 10^{-4}$ .

When allowing the Yukawa couplings to be complex, the 95%-CL bound changes to

$$0.76 \lesssim |1 - (0.2 Y_{sb}^2 + 1.1 \bar{Y}_{sb}^2) \times 10^6| \lesssim 1.29. \quad (26)$$

In this case, several new effects show up. The phase  $\phi_s \equiv \arg(M_{12}^s)$  for  $B_s$ - $\bar{B}_s$  mixing will acquire a non-vanishing NP piece, and this will affect the parameter  $\mathcal{A}_{\Delta\Gamma}$ . We have carried out a numerical analysis considering experimental bounds from these quantities. As an illustration, we take  $(Y_{sb}, Y_{\mu\mu}, \bar{Y}_{\mu\mu}) = (0, \lambda_\mu, \lambda_\mu)$  and obtain the bounds on the phase  $\bar{\theta}_{sb}$  and the magnitude of  $\bar{Y}_{sb}$  from the  $B_s \rightarrow \mu^+\mu^-$  decay and  $B_s$ - $\bar{B}_s$  mixing. Fig. 3 shows the allowed parameter space for  $(\bar{\theta}_{sb}, |\bar{Y}_{sb}|)$  and the corresponding regions of  $\mathcal{A}_{\Delta\Gamma}$  and  $\phi_s$ . As can be seen in Eq. (15), the Higgs FCNC effects on  $\mathcal{A}_{\Delta\Gamma}$  become significant for  $\bar{\theta}_{sb} \approx \pm\pi/2$  under the current assumption of  $Y_{sb} = 0$ . As the SM contribution has an almost null phase in  $M_{12}^s$ ,  $\phi_s$  has a significant modification when  $\bar{\theta}_{sb} \approx \pm\pi/4$  or  $\pm 3\pi/4$ . Since we have included the constraints from the CP phase  $\phi_s^{c\bar{c}s} = -0.03 \pm 0.033$  radian [21], the regions

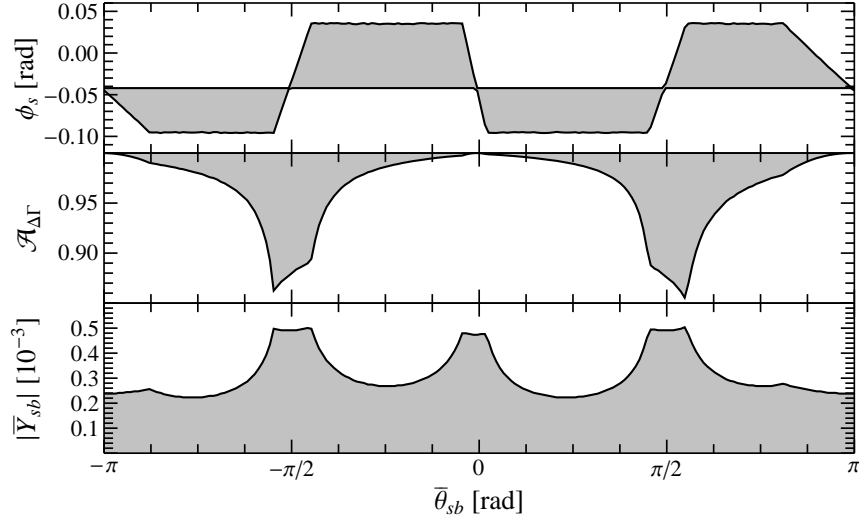


FIG. 3: Allowed parameter space of  $(\bar{\theta}_{sb}, |\bar{Y}_{sb}|)$ , as constrained by the  $B_s \rightarrow \mu^+ \mu^-$  and  $B_s$ - $\bar{B}_s$  mixing at 95% CL under the assumption of  $(Y_{sb}, Y_{\mu\mu}, \bar{Y}_{\mu\mu}) = (0, \lambda_\mu, \lambda_\mu)$ . The corresponding allowed regions for  $\mathcal{A}_{\Delta\Gamma}$  and  $\phi_s$  are also given.

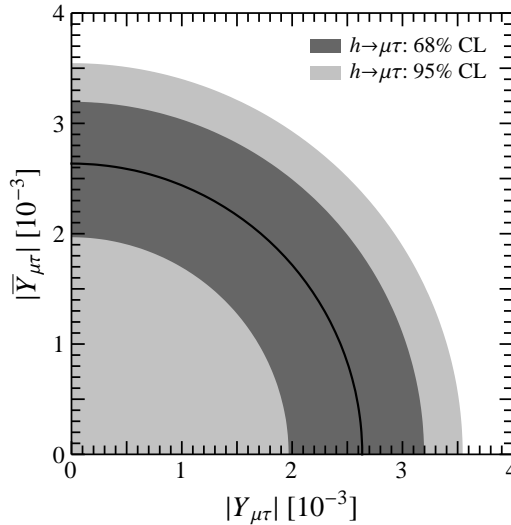


FIG. 4: Constraints in the  $(|Y_{\mu\tau}|, |\bar{Y}_{\mu\tau}|)$  plane. The black circular curve reproduces the central value of the CMS  $h \rightarrow \mu\tau$  data. The dark and light shaded regions correspond respectively to the regions of  $1\sigma$  and 95% CL.

near  $\bar{\theta}_{sb} \approx \pm\pi/4, \pm 3\pi/4$  are more strongly constrained.

Recently, with the  $19.7 \text{ fb}^{-1}$  data, the CMS Collaboration has determined that  $\mathcal{B}(h \rightarrow \mu\tau) = (0.84_{-0.37}^{+0.39})\%$  or  $< 1.51\%$  at the 95% CL [22]. With the  $20.3 \text{ fb}^{-1}$  data, the ATLAS

Collaboration has also found a less significant result that  $\mathcal{B}(h \rightarrow \mu\tau) = (0.53 \pm 0.51)\%$  or  $< 1.43\%$  at the 95% CL [23]. The central values are substantially larger than the SM prediction. Since the error on the ATLAS data is too large, we will take only the CMS measurement as our constraint. Here the complex  $Y_{\mu\tau}$  and  $\bar{Y}_{\mu\tau}$  can contribute to the  $h \rightarrow \tau\mu$  decay at tree level, and one has from the CMS data [22]

$$\sqrt{|Y_{\mu\tau}|^2 + |\bar{Y}_{\mu\tau}|^2} < 3.6 \times 10^{-3} \quad (27)$$

at 95% CL, shown in Fig. 4. The black solid curve reproduces the central value of the CMS observation, the dark shaded region indicates the  $1\sigma$  range, and the light shaded region covers the region of 95% CL.

#### IV. DISCUSSIONS

In the previous section, we have shown that the precision measurements of the  $B_s \rightarrow \mu^+\mu^-$  decay and  $\Delta m_s$  have tightly restricted the allowed ranges of some tree-level Higgs FCNC interactions. With the input of  $h \rightarrow \mu\tau$  decay width, we have also obtained restraints in a couple of lepton FCNC Yukawa couplings. It is remarkable that flavor physics has now become a precision test ground for the study of Higgs properties. We now discuss the implications of the above-mentioned constraints in other rare decay processes.

##### A. The $h \rightarrow sb$ , $B_s \rightarrow \tau\tau$ , and $B_s \rightarrow \mu\tau$ decays

In the SM, the Higgs total decay width  $\Gamma_h^{\text{SM}} \simeq 4.1$  MeV. This can be modified if the  $h \rightarrow sb$  and  $\mu\tau$  decay considered in this work contribute significantly. Using the constraint Eq. (26) obtained for the generally complex Yukawa couplings in Section II B, we have

$$\Gamma(h \rightarrow sb) < 0.11 \text{ MeV} \quad \text{or} \quad \mathcal{B}(h \rightarrow sb) < 2.7\% \quad (28)$$

at 95% CL. Note that here we only consider the scenario where the SM contribution dominates in the estimate of  $\Delta m_s$ . With such a small decay rate and only one  $b$  quark for tagging, the channel is expected to be very difficult to measure at the LHC.

The  $B_s \rightarrow \tau^+\tau^-$  decay rate calculation is similar to that of the  $B_s \rightarrow \mu^+\mu^-$  decay. Using experimental  $h \rightarrow \tau\tau$  data and constraints on the generally complex  $Y_{sb}$  and  $\bar{Y}_{sb}$  from  $B_s - \bar{B}_s$

mixing, we find

$$0.5 \text{ (0.3)} < \frac{\mathcal{B}(B_s \rightarrow \tau^+ \tau^-)}{\mathcal{B}(B_s \rightarrow \tau^+ \tau^-)_{\text{SM}}} < 1.8 \text{ (2.2)} \quad (29)$$

at  $1\sigma$  level (95% CL).

In the SM, the  $B_s \rightarrow \mu\tau$  decay is suppressed because its leading-order process occurs at the one-loop level. However, with the FCNC couplings assumed in Eq. (6), this decay process happens at tree level through the mediation of the Higgs boson. Again, by scanning the allowed parameter space given in Eqs. (26) and (27), we find that  $\mathcal{B}(B_s \rightarrow \mu\tau)$  can be as large as  $1.5 \text{ (3.1)} \times 10^{-8}$  at  $1\sigma$  level (95% CL). The 95%-CL upper limit is about one order of magnitude larger than the currently measured  $B_s \rightarrow \mu^+ \mu^-$  decay branching ratio.

### B. Leptonic decays of $B_s$ and $h$ with the Cheng-Sher ansatz

As mentioned earlier, the flavor-conserving and flavor-changing components of the scalar and pseudoscalar Yukawa couplings  $Y$  and  $\bar{Y}$  are generally independent. To improve the predictive power, one can assume some specific relations among the couplings. One popular scenario is the Cheng-Sher ansatz [27]. One can apply the Cheng-Sher ansatz to the quark and lepton sectors separately. As an illustration, here we will work with only applying the Cheng-Sher ansatz to the charged leptons to see how some predictions can be made. In this case, the charged lepton Yukawa couplings take the following form

$$Y_{ij} = \xi_\ell \frac{\sqrt{2m_i m_j}}{v} \quad \text{and} \quad \bar{Y}_{ij} = \bar{\xi}_\ell \frac{\sqrt{2m_i m_j}}{v}, \quad (30)$$

where  $\xi_\ell$  and  $\bar{\xi}_\ell$  are presumably  $\mathcal{O}(1)$  parameters.

In the following, we will apply this ansatz and take into account the  $h \rightarrow \mu\tau$  decay branching ratio,  $\mathcal{B}(h \rightarrow \mu\tau)_{\text{CMS}} = (0.84_{-0.37}^{+0.39})\%$ , measured by the CMS Collaboration [22] and the signal strength of the  $h \rightarrow \tau\tau$  channel,  $\mu_{\tau\tau} = 1.11_{-0.22}^{+0.24}$  [26]. We will also use Eq. (22) to predict the flavor-changing  $h \rightarrow sb$  decay rate.

With the Cheng-Sher ansatz in the lepton sector, the constraints on  $(Y_{\mu\tau}, \bar{Y}_{\mu\tau})$  from the CMS data can be converted to the constraints on  $(\xi_\ell, \bar{\xi}_\ell)$ , as shown in Fig. 5, where the subscript  $\ell$  refers to the charged leptons. In this figure, the parameter regions allowed by the  $h \rightarrow \tau\tau$  measurement from the combined Run-I data and the CMS best fit value of  $\mathcal{B}(h \rightarrow \tau\mu)$  are respectively given by the dark gray ring and light gray circular areas, both at

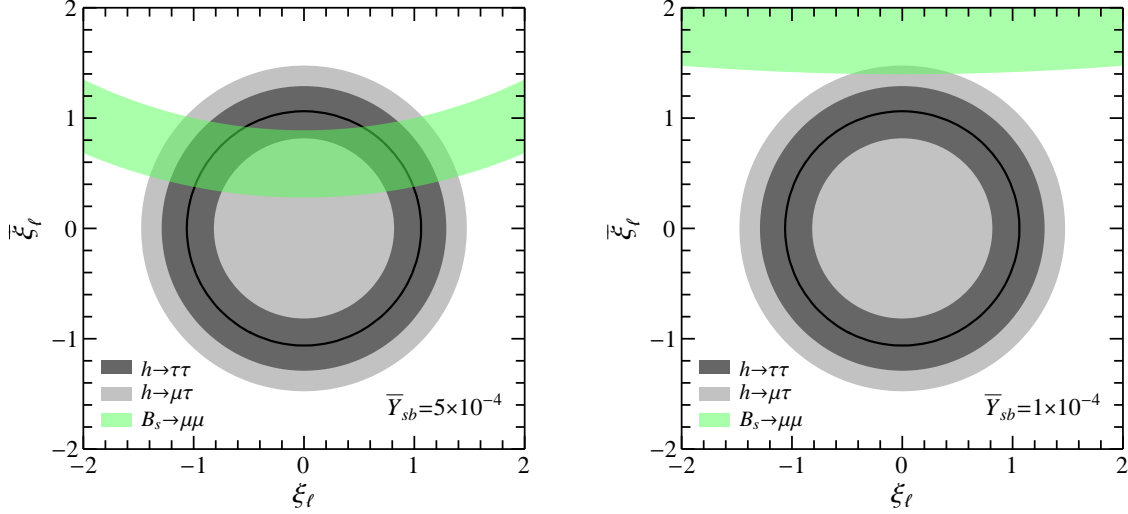


FIG. 5: Combined constraints on  $(\xi_\ell, \bar{\xi}_\ell)$  under the Cheng-Sher ansatz. The dark and light gray regions are respectively the parameter space allowed by the  $h \rightarrow \tau\tau$  measurement from the combined Run-I data and the CMS  $h \rightarrow \mu\tau$  data at 95% CL. The black circle reproduces the central value of the  $h \rightarrow \mu\tau$  data. In the case of  $\bar{Y}_{sb} = 5 \times 10^{-4}$  (left plot) and  $\bar{Y}_{sb} = 1 \times 10^{-4}$  (right plot), the parameter space  $(\xi_\ell, \bar{\xi}_\ell)$  satisfying  $0.7 < \mathcal{B}(B_s \rightarrow \mu^+\mu^-)/\mathcal{B}(B_s \rightarrow \mu^+\mu^-)_{\text{SM}} < 0.9$  are shown by the green region.

95% CL. The former covers the black circle that reproduces the central value of  $\mathcal{B}(h \rightarrow \tau\mu)$ . Furthermore, as discussed in the previous section, the largest allowed  $|\bar{Y}_{sb}|$  is about  $5 \times 10^{-4}$ . We take  $\bar{Y}_{sb} = 5 \times 10^{-4}$  (left plot) and  $1 \times 10^{-4}$  (right plot) as two benchmark values, and find the region in the  $(\xi_\ell, \bar{\xi}_\ell)$  plane that reduces  $\mathcal{B}(B_s \rightarrow \mu^+\mu^-)_{\text{SM}}$  by 10% to 30%, to be in better agreement with the current data. It is shown that, unless for a very small  $\bar{Y}_{sb}$ , the Higgs FCNC couplings under the Cheng-Sher ansatz can simultaneously generate the observed  $h \rightarrow \tau\mu$  decay rate while suppressing the  $B_s \rightarrow \mu^+\mu^-$  branching ratio by  $\sim 20\%$ . By varying  $\bar{Y}_{sb}$  until there is no overlap between the region allowed by the  $h \rightarrow \mu\tau$  and  $\tau\tau$  data and the region for 10% to 30% reduction from  $\mathcal{B}(B_s \rightarrow \mu^+\mu^-)_{\text{SM}}$ , one can obtain a lower bound on  $|\bar{Y}_{sb}|$ , as can be seen by comparing the left and right plots of Fig. 5. This exercise shows that if  $\mathcal{B}(B_s \rightarrow \mu^+\mu^-)$  can be better determined and seen to be significantly lower than the SM prediction, a lower bound on the pseudoscalar FCNC Yukawa coupling  $|\bar{Y}_{sb}|$  can be obtained. This lower bound becomes larger if one concentrates on the region where  $\xi \sim 1$  and  $\bar{\xi} \sim 0$ , close to the case of SM-like flavor-conserving Yukawa couplings.

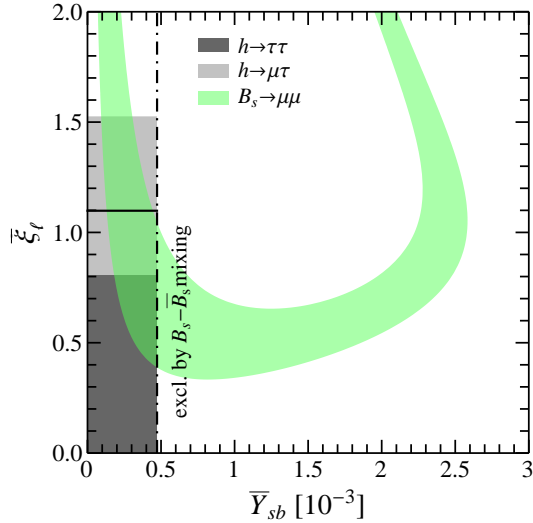


FIG. 6: Combined constraints on  $(\bar{Y}_{sb}, \bar{\xi}_\ell)$  under the Cheng-Sher ansatz in the case of the SM scalar Yukawa couplings  $Y_{ij}$ . The dot-dashed line denotes the upper bound from  $\Delta m_s$ . The plotting style is the same as in Fig. 5.

The experimental data on  $h \rightarrow \tau\tau$  play an important role in excluding the central region in Fig. 5.

We note in passing that for the overlapped region between the green region and the light gray region in Fig. 5 and assuming that the up-type quarks have only the SM Yukawa couplings, the measured signal strengths of different Higgs decay channels are modified because the changes in their branching ratios. The predictions under the Cheng-Sher ansatz are consistent with the current measurements.

As an illustration, consider the scenario where  $Y_{sb} = 0$  and the Cheng-Sher ansatz is applied to the pseudoscalar Yukawa couplings of the charged leptons. We also suppose that  $\mathcal{B}(B_s \rightarrow \mu^+\mu^-)$  will be measured with high precision and determined to fall between 70% and 90% of its SM expectation. Fig. 6 shows the combined constraints in the  $(\bar{Y}_{sb}, \bar{\xi}_\ell)$  plane. The region to the left of the dot-dashed line is ruled out by  $\Delta m_s$  at 95% CL. At the 95% CL,  $\bar{\xi}_\ell$  is restricted to a region between 0.4 and 0.8, which, however, can not reproduce the central value of the CMS  $h \rightarrow \mu\tau$  data.

As mentioned in Section II C, we would like to make a comment on the possibility of observing CP violation in  $h \rightarrow \tau\bar{\tau}$  through the operator  $\mathcal{O}_\pi = \vec{p}_\tau \cdot (\vec{p}_{\pi^+} \times \vec{p}_{\pi^-})$ . Taking  $\bar{Y}_{sb} = 5 \times 10^{-4}$ , as in the left plot of Fig. 5, one can infer using the Cheng-Sher ansatz for

$Y_{\tau\tau}$  and  $\bar{Y}_{\tau\tau}$  that the absolute value of  $A_\pi$ , defined in Eq. (23), can be almost as large as the maximally allowed value of  $\pi/8$ . This can be tested at a Higgs factory.

If one also applies the Cheng-Sher ansatz to the down-type quarks, rough estimates of the Higgs FCNC contributions to  $\Delta m_K^{\text{NP}}$  and  $\Delta m_{B_d}^{\text{NP}}$  can be made once  $\Delta m_{B_s}^{\text{NP}}$  is known, using

$$\Delta m_K^{\text{NP}} \approx \frac{R_K}{R_{B_s}} \frac{f_K^2 m_K}{f_{B_s}^2 m_{B_s}} \frac{m_d}{m_b} \Delta m_s^{\text{NP}}$$

and

$$\Delta m_d^{\text{NP}} \approx \frac{R_{B_d}}{R_{B_s}} \frac{f_{B_d}^2 m_{B_d}}{f_{B_s}^2 m_{B_s}} \frac{m_d}{m_s} \Delta m_s^{\text{NP}},$$

where  $R_K/R_{B_s} \simeq 12.6$  and  $R_{B_d}/R_{B_s} \simeq 1$  [36], and the last fractions in both expressions come from the ansatz. Assuming  $\Delta m_s^{\text{NP}}$  to be about 10% of the experimental value, we find that the contributions to  $\Delta m_K^{\text{NP}}$  is about 20% of its experimental value, but with opposite sign for real Yukawa couplings. With complex Yukawa couplings, the contribution from the imaginary part will add to the SM predicted value and become closer to the experimental value. Since there is a large uncertainty caused by long distance contribution for  $\Delta m_K$  [44–47], it is possible that when adding all contributions together the correct value will be produced and the Cheng-Sher ansatz is valid here. The contributions to  $\Delta m_d^{\text{NP}}$  is also about 10%. Therefore within the region allowed by the  $B_s$ - $\bar{B}_s$  mixing, the  $B_d$ - $\bar{B}_d$  is predicted to be consistent with the data. As a consequence, the  $B_d \rightarrow \mu^+ \mu^-$  decay branching ratio will also be about the same order as that in the SM, which is smaller than the current experimental bound of  $3.4 \times 10^{-10}$  at 95% CL [17]. One also predicts  $\mathcal{B}(B_d \rightarrow \mu\tau)/\mathcal{B}(B_s \rightarrow \mu\tau) \approx m_d/m_s$  resulting in  $\mathcal{B}(B_d \rightarrow \mu\tau) < 1.5 \times 10^{-9}$ . This is much smaller than current experimental bound of  $2.2 \times 10^{-5}$ .

## V. SUMMARY

Motivated by the recent precision determination of the  $B_s \rightarrow \mu^+ \mu^-$  decay branching ratio, we consider its constraints on tree-level flavor-changing Yukawa couplings with the 125-GeV Higgs boson, as defined in Eq. (6). To gain more definite information, we also take into account the  $B_s$  mass difference  $\Delta m_s$ , the  $h \rightarrow \mu\tau$  decay branching ratio determined by the CMS Collaboration, and the signal strength of the  $h \rightarrow \tau^+ \tau^-$  channel from the LHC Run-I data.

In what follows, we summarize the constraints on flavor-changing couplings obtained in this work, assuming that they are generally complex. From  $\overline{\mathcal{B}}(B_s \rightarrow \mu^+\mu^-)$  alone, we obtain

$$0.66 \lesssim |5.6 \times 10^5 \bar{Y}_{sb} Y_{\mu\mu}|^2 + |1 - 6.0 \times 10^5 \bar{Y}_{sb} \bar{Y}_{\mu\mu}|^2 \lesssim 1.26 .$$

From  $\Delta m_s$ , we have

$$0.76 \lesssim |1 - (0.2 Y_{sb}^2 + 1.1 \bar{Y}_{sb}^2) \times 10^6| \lesssim 1.29 .$$

Combining with the constraints from the  $h \rightarrow \mu\tau$  branching ratio measured by the CMS Collaboration and the  $h \rightarrow \tau\tau$  signal strength from the LHC Run-I data, we have made predictions for the branching ratios of  $B_s \rightarrow \mu\tau$ ,  $\tau\tau$  and  $h \rightarrow sb$  decays. In particular,  $\mathcal{B}(B_s \rightarrow \mu\tau)$  can be as large as  $3.1 \times 10^{-8}$  at 95% CL. This may be quite challenging for the LHCb and future Belle-II experiments to measure.

Finally, we use the above-mentioned constraints obtained from data to test the Cheng-Sher ansatz. We have shown that if the  $B_s \rightarrow \mu^+\mu^-$  branching ratio is found to deviate significantly from the SM expectation in the future, the combined analysis with the  $h \rightarrow \tau\tau$  and  $\mu\tau$  data can give us a lower bound on the pseudoscalar Yukawa coupling  $\bar{Y}_{sb}$ , provided that the  $B_s$  mass difference is still dominated by the SM contribution. As an example, the parameter  $\bar{\xi}_\ell$  is found to fall within the  $\mathcal{O}(1)$  regime when the scalar Yukawa couplings are assumed to be SM-like. We have also made a brief comment on the possibility of observing CP violation in the  $h \rightarrow \tau^+\tau^-$  decay.

## Acknowledgments

CWC was supported in part by the Ministry of Science and Technology (MOST) of ROC (Grant No. MOST 104-2628-M-002-014-MY4). XGH was supported in part by MOE Academic Excellent Program (Grant No. 105R891505) and MOST of ROC (Grant No. MOST 104-2112-M-002-015-MY3), and in part by NSFC of PRC (Grant No. 11575111). This work was also supported by Key Laboratory for Particle Physics, Astrophysics and Cosmology, Ministry of Education, and Shanghai Key Laboratory for Particle Physics and Cosmology (SKLPPC) (Grant No. 11DZ2260700).

---

[1] S. L. Glashow, Nucl. Phys. **22**, 579 (1961).

- [2] S. Weinberg, Phys. Rev. Lett. **19**, 1264 (1967).
- [3] A. Salam, Conf. Proc. C **680519**, 367 (1968).
- [4] F. Englert and R. Brout, Phys. Rev. Lett. **13**, 321 (1964).
- [5] P. W. Higgs, Phys. Rev. Lett. **13**, 508 (1964).
- [6] G. S. Guralnik, C. R. Hagen and T. W. B. Kibble, Phys. Rev. Lett. **13**, 585 (1964).
- [7] G. Aad *et al.* [ATLAS Collaboration], Phys. Lett. B **716**, 1 (2012) [arXiv:1207.7214 [hep-ex]].
- [8] S. Chatrchyan *et al.* [CMS Collaboration], Phys. Lett. B **716**, 30 (2012) [arXiv:1207.7235 [hep-ex]].
- [9] G. C. Branco, P. M. Ferreira, L. Lavoura, M. N. Rebelo, M. Sher and J. P. Silva, Phys. Rept. **516**, 1 (2012) [arXiv:1106.0034 [hep-ph]]; C. W. Chiang, N. G. Deshpande, X. G. He and J. Jiang, Phys. Rev. D **81**, 015006 (2010) [arXiv:0911.1480 [hep-ph]]; X. G. He and G. Valencia, Phys. Rev. D **66**, 013004 (2002) Erratum: [Phys. Rev. D **66**, 079901 (2002)] [hep-ph/0203036].
- [10] S. L. Glashow and S. Weinberg, Phys. Rev. D **15**, 1958 (1977).
- [11] A. Pich and P. Tuzon, Phys. Rev. D **80**, 091702 (2009) [arXiv:0908.1554 [hep-ph]].
- [12] W. Altmannshofer, P. Paradisi and D. M. Straub, JHEP **1204**, 008 (2012) [arXiv:1111.1257 [hep-ph]].
- [13] K. De Bruyn, R. Fleischer, R. Knegjens, P. Koppenburg, M. Merk, A. Pellegrino and N. Tuning, Phys. Rev. Lett. **109**, 041801 (2012) [arXiv:1204.1737 [hep-ph]].
- [14] R. Fleischer, Nucl. Phys. Proc. Suppl. **241-242**, 135 (2013) [arXiv:1208.2843 [hep-ph]].
- [15] A. J. Buras, R. Fleischer, J. Girschbacher and R. Knegjens, JHEP **1307**, 77 (2013) [arXiv:1303.3820 [hep-ph]].
- [16] W. Altmannshofer, C. Niehoff and D. M. Straub, arXiv:1702.05498 [hep-ph].
- [17] R. Aaij *et al.* [LHCb Collaboration], arXiv:1703.05747 [hep-ex].
- [18] S. Chatrchyan *et al.* [CMS Collaboration], Phys. Rev. Lett. **111**, 101804 (2013) [arXiv:1307.5025 [hep-ex]].
- [19] C. Bobeth, M. Gorbahn, T. Hermann, M. Misiak, E. Stamou and M. Steinhauser, Phys. Rev. Lett. **112**, 101801 (2014) [arXiv:1311.0903 [hep-ph]].
- [20] M. Artuso, G. Borissov and A. Lenz, Rev. Mod. Phys. **88**, no. 4, 045002 (2016) [arXiv:1511.09466 [hep-ph]].
- [21] Y. Amhis *et al.*, arXiv:1612.07233 [hep-ex].

- [22] V. Khachatryan *et al.* [CMS Collaboration], Phys. Lett. B **749**, 337 (2015) [arXiv:1502.07400 [hep-ex]].
- [23] G. Aad *et al.* [ATLAS Collaboration], Eur. Phys. J. C **77**, no. 2, 70 (2017) [arXiv:1604.07730 [hep-ex]].
- [24] A. J. Buras, F. De Fazio, J. Girrbach, R. Kneegjens and M. Nagai, JHEP **1306**, 111 (2013) doi:10.1007/JHEP06(2013)111 [arXiv:1303.3723 [hep-ph]].
- [25] R. Harnik, J. Kopp and J. Zupan, JHEP **1303**, 026 (2013) [arXiv:1209.1397 [hep-ph]].
- [26] G. Aad *et al.* [ATLAS and CMS Collaborations], JHEP **1608**, 045 (2016) [arXiv:1606.02266 [hep-ex]].
- [27] T. P. Cheng and M. Sher, Phys. Rev. D **35**, 3484 (1987).
- [28] G. Buchalla, A. J. Buras and M. E. Lautenbacher, Rev. Mod. Phys. **68**, 1125 (1996) [hep-ph/9512380].
- [29] G. Buchalla and A. J. Buras, Nucl. Phys. B **400**, 225 (1993).
- [30] M. Misiak and J. Urban, Phys. Lett. B **451**, 161 (1999) [hep-ph/9901278].
- [31] G. Buchalla and A. J. Buras, Nucl. Phys. B **548**, 309 (1999) [hep-ph/9901288].
- [32] C. Bobeth, M. Gorbahn and E. Stamou, Phys. Rev. D **89**, no. 3, 034023 (2014) [arXiv:1311.1348 [hep-ph]].
- [33] T. Hermann, M. Misiak and M. Steinhauser, JHEP **1312**, 097 (2013) [arXiv:1311.1347 [hep-ph]].
- [34] X. Q. Li, J. Lu and A. Pich, JHEP **1406**, 022 (2014) [arXiv:1404.5865 [hep-ph]].
- [35] X. D. Cheng, Y. D. Yang and X. B. Yuan, Eur. Phys. J. C **76**, no. 3, 151 (2016) [arXiv:1511.01829 [hep-ph]].
- [36] A. J. Buras, S. Jager and J. Urban, Nucl. Phys. B **605**, 600 (2001) [hep-ph/0102316].
- [37] A. J. Buras, hep-ph/9806471.
- [38] N. Carrasco *et al.* [ETM Collaboration], JHEP **1403**, 016 (2014) [arXiv:1308.1851 [hep-lat]].
- [39] A. Bazavov *et al.* [Fermilab Lattice and MILC Collaborations], Phys. Rev. D **93**, no. 11, 113016 (2016) [arXiv:1602.03560 [hep-lat]].
- [40] X. G. He, J. P. Ma and B. McKellar, Mod. Phys. Lett. A **9**, 205 (1994) [hep-ph/9302230]; A. Hayreter, X. G. He and G. Valencia, Phys. Lett. B **760**, 175 (2016) [arXiv:1603.06326 [hep-ph]]; A. Hayreter, X. G. He and G. Valencia, Phys. Rev. D **94**, no. 7, 075002 (2016) [arXiv:1606.00951 [hep-ph]].

- [41] C. Patrignani *et al.* [Particle Data Group], *Chin. Phys. C* **40**, no. 10, 100001 (2016).
- [42] J. Charles *et al.* [CKMfitter Group], *Eur. Phys. J. C* **41**, no. 1, 1 (2005) [hep-ph/0406184].
- [43] S. Aoki *et al.*, *Eur. Phys. J. C* **77**, no. 2, 112 (2017) [arXiv:1607.00299 [hep-lat]].
- [44] V. Antonelli, S. Bertolini, M. Fabbrichesi and E. I. Lashin, *Nucl. Phys. B* **493**, 281 (1997) [hep-ph/9610230].
- [45] S. Bertolini, J. O. Eeg, M. Fabbrichesi and E. I. Lashin, *Nucl. Phys. B* **514**, 63 (1998) [hep-ph/9705244].
- [46] A. J. Buras, D. Guadagnoli and G. Isidori, *Phys. Lett. B* **688**, 309 (2010) [arXiv:1002.3612 [hep-ph]].
- [47] A. J. Buras, J. M. Grard and W. A. Bardeen, *Eur. Phys. J. C* **74**, 2871 (2014) [arXiv:1401.1385 [hep-ph]].